Available online at www.sciencedirect.com
SCIENCE DIRECT®
Journal of Luminescence 119–120 (2006) 198–203
JOURNAL OF LUMINESCENCE
www.elsevier.com/locate/jlumin

Carrier transfer and magneto-transport in single modulation-doped V-grooved quantum wire modified by ion implantation

S.H. Huang[a], Zhanghai Chen[a,*], F.Z. Wang[a], S.C. Shen[a], H.H. Tan[b], L. Fu[b], M. Fraser[b], C. Jagadish[b]

[a]*Surface Physics Laboratory, Department of Physics, Fudan University, Shanghai 200433, China*
[b]*Department of Electronic Material Engineering, Research School of Physical Science and Engineering, Australian National University, Canberra, ACT 0200, Australia*

Available online 28 February 2006

Abstract

A single $Al_{0.5}Ga_{0.5}As/GaAs$ V-grooved quantum wire modified by selective ion implantation and rapid thermal annealing was investigated by using spatially resolved micro-photoluminescence spectroscopy and magneto-resistance measurements. The results of spatially resolved photoluminescence indicate that the ion-implantation-induced quantum well intermixing significantly raises the electronic sub-band energies in the side quantum wells (SQWs) and vertical quantum wells, and a more efficient accumulation of electrons in the quantum wires is achieved. Processes of real space carrier transfer from the SQW to the quantum wire was experimentally observed, and showed the blocking effect of carrier transfer due to the existence of the necking quantum well region. Furthermore, magneto-transport investigation on the ion-implanted quantum wire samples shows the quasi-one-dimensional intrinsic motion of electrons, which is important for the design and the optimization of one-dimensional electronic devices.

PACS: 73.21.Hb; 73.50.Dn; 73.63.Nm

Keywords: Quantum wire; Carrier transfer; Magneto-transport; Ion implantation

1. Introduction

Recently, there is considerable interest in the fabrication and study of quasi-one-dimensional (quasi-1D) quantum wires (QWRs) due to their potential application for novel optoelectronic devices such as QWR laser array [1,2], etc. Among the various techniques developed for producing quasi-1D QWRs, the self-organized growth on patterned substrates has been proven to be one of the most promising methods, due to the simplicity

*Corresponding author. Tel./fax: +86 21 55664193.
E-mail address: zhanghai@fudan.edu.cn (Z. Chen).

0022-2313/$ - see front matter © 2006 Elsevier B.V. All rights reserved.
doi:10.1016/j.jlumin.2005.12.061

of fabrication [3–5]. The QWR is fabricated by direct epitaxial growth on a V-grooved GaAs substrate. However, due to the nonplanar property of the substrate and enhanced mobility of Ga atoms compared to that of Al atoms, some complicated surrounding nanostructures near the QWRs, such as vertical quantum wells (VQWLs), side quantum wells (SQWLs), are also formed during the wire formation process [6]. These additional structures decrease the electron capture efficiency in the QWR region and therefore make the observation and investigation of pure-1D behaviors of the QWR more difficult. Due to the relative large volume of the quantum well regions in comparison with the wire region in the V-grooved structure, emissions from the well regions usually prevent clear observation of the emission from the wire region, particularly for a narrower wire structure. To suppress the emission from the additional structures and get better confinement of the electrons in QWRs, a technique for post-growth modification of the materials is required. We used selective ion implantation of certain dose, followed by rapid thermal annealing (RTA) to improve the quantum confinement of QWRs [7]. This enhances significantly the optical emission from QWR, which was confirmed by the spatially resolved photoluminescence (PL) measurements. The results indicate that the selective ion-implantation-induced quantum well interdiffusion reduces the efficiency of the photon emission from the implanted well regions due to irradiation damage, and therefore results in an efficient carrier capture in the wire. Furthermore, the magneto-transport properties of the ion-implanted QWRs were also investigated. Clear quasi-1D transport behaviors, which are of considerable importance for the design and optimization of 1D electronic devices, were also observed.

2. Experiments

The QWR samples were grown by low-pressure metal-organic chemical vapor deposition at 700 °C in a horizontal reactor on a GaAs (1 0 0) semi-insulating substrate. The substrate was patterned with standard photolithography and wet etching to form an array of V-grooves of 4 μm pitch oriented along the [0 1 −1] direction. The epitaxial layer consists of a 0.2 μm undoped GaAs buffer layer, a 1 μm undoped $Al_{0.5}Ga_{0.5}As$ barrier layer followed by a Si-doped layer, a 10 nm undoped $Al_{0.5}Ga_{0.5}As$ spacer layer, a 6 nm undoped GaAs layer, a 0.2 μm undoped $Al_{0.5}Ga_{0.5}As$ upper layer. A 10 nm GaAs cap layer was finally grown. At the bottom of the V-grooves, GaAs QWR were formed.

After the growth, a self-aligned dual implantation technique was used to selectively intermix the SQWLs with As^+ ions of 500 keV at various doses and room temperature. The ion beam was arranged to be $\pm 50^\circ$ tilted from the substrate vertical direction as shown in Fig. 1, so that the wires were not irradiated. After the ion implantation, the samples were thermally annealed in an argon ambient at 900 °C for 30 s in a RTA chamber with GaAs proximity cap.

A spatially resolved PL spectrometer equipped with a microscope was used to measure the micro-PL spectra of QWR samples, by which the excitation laser spot can be focused to about 1 μm in diameter, and the excitation wavelength was 633 nm.

The magneto-transport measurements were carried out on the samples at 4.2 K. The Ohmic contacts on wires are fabricated by evaporating Au–Ge film on the samples followed by RTA at 400 °C. The separation between the contacts is 500 μm.

3. Results and discussion

3.1. Spatially resolved PL from QWR

In order to resolve and identify the photo-response from a single quantum wire, we have employed the micro-PL spectrometer to measure the PL spectra of QWR samples at room temperature. Fig. 2 is the micro-PL spectra obtained at room temperature by scanning the excitation light spot across a single QWR. The spectra show the PL signals from different regions of the sample. The PL from individual quantum

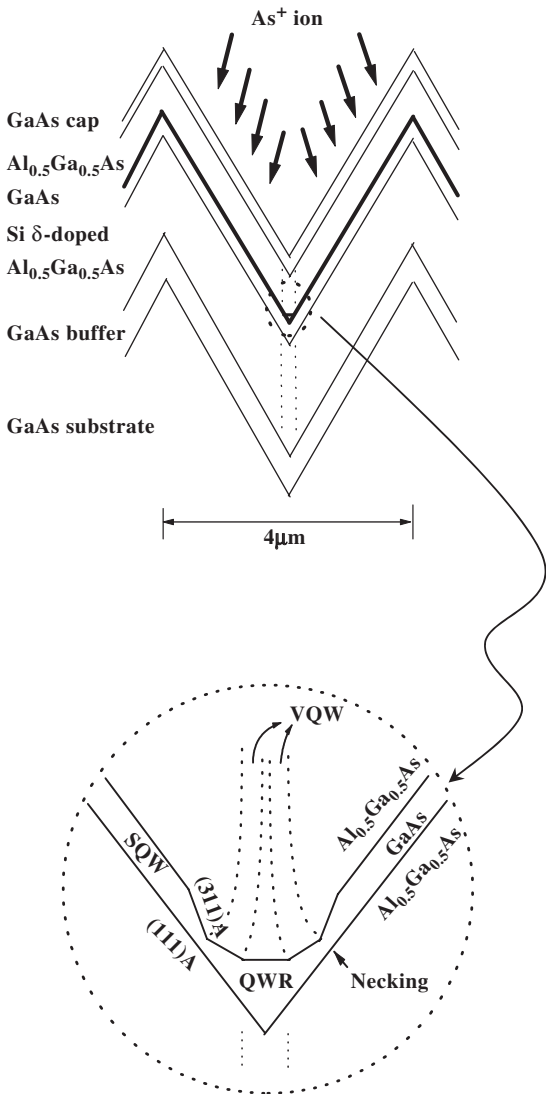

Fig. 1. Schematic structure of the V-groove QWR.

wire which may not be resolved in conventional PL measurements, is easily identified.

When the excitation spot is focused on the unpatterned region, the emissions locate at 1.637 and 1.420 eV (this peak is from GaAs substrate). When the excitation spot is focused on the patterned region, the PL peaks appear at 1.572, 1.668 and 1.760 eV. Spatial scanning across a single V-groove indicates that the 1.572, 1.668 and 1.760 eV PL peaks are from the QWR, SQWL, and VQWL, respectively [8]. They are attributed to the transitions between the first heavy hole sub-level (1hh) and the first electron sublevel (1e) in the QWR, SQWL, and VQWL, respectively. The QWR PL emission at 1.572 eV is consistent with the theoretical expectation [9] of $E_{1hh-1e} = 1.5713$ eV for the QWR with the wire width of 20 nm.

Fig. 3 shows the micro-PL spectra obtained from the quantum wire regions and SQW regions at room temperature for the samples implanted with different dose density of As^+ ion. The assignments of the peaks are indicated in the figures. No characteristic PL signal from the quantum wire can be seen for the as-grown sample. However, after the ion implantation, the PL response from the QWR appears and its intensity is enhanced monotonously with increasing the dose density. For the VQWL and SQWL, their PL intensities increase at first with ion implantation, and then decrease rapidly with further intensifying the ion beam. The reason for the ion-implantation-enhanced quantum wire PL signal is that the interface intermixing, which is induced by As^+ ion-implantation, increases the sub-band energies of the SQWL and VQWL and thus reduces the carrier confinement in these regions. This conclusion can be confirmed by the significant blue shift and intensity suppressing of the SQWL and VQWL PL peaks, as shown in Fig. 3 and its insets. This blue shift is caused by the interface intermixing, which is very useful to increase the confinement of carriers in the QWR region for optoelectronic device application. Furthermore, since the QWR are unimplanted and less affected by the RTA process due to its larger thickness, more photo-generated carriers could relax into the quantum wire before they recombine in the SQWL and VQWL. From the above investigation, it is clearly shown that the selective ion implantation will effectively decrease the number of carriers occupied in the SQWL and VQWL.

3.2. Carrier transfer from SQWL to QWR

The lateral confinement of QWR is caused by the necking quantum well region, which blocks the

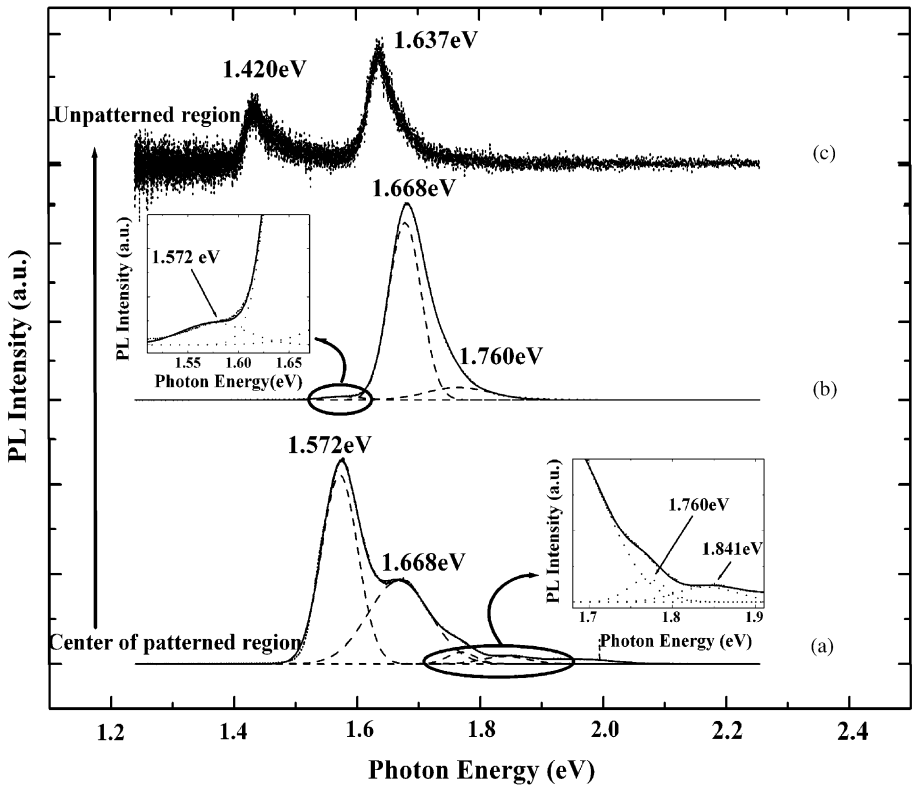

Fig. 2. PL spectra with different optical excitation positions, with excitation spots scanning away from the V-grooved region to the unpatterned regions, excited with the 633 nm line of an He–Ne laser. The QWR sample with the ion implantation dose density of $10^{13}\,cm^{-2}$. (a)–(c) correspond to the beam spots focusing on the QWR region, the top quantum well and the unpatterned QWL, respectively. The solid line is the fitting curve and the dots are the experimental data, the dash lines are the involved individual transition.

carrier transfer from the SQWL to the QWR region. The blocking effect on the carrier transfer process from the SQWL to the QWR by the necking region is directly observed by injecting the carriers into the small SQWL region at very low carrier density. By observing the carriers trapping process from the SQWL to the QWR, we can prove whether the necking region exists or not in QWR samples treated by ion implantation.

Fig. 4 shows the evolution of the spectra with the excitation power density at 4 K. When the laser beam of 1.8 W/cm^2 focus onto the SQWL region, only two pronounced emissions could be observed, which were from the SQWL and the VQWL. With increasing the excitation power intensity to 181 W/cm^2, the emission from the QWR could be observed, because of many carriers injecting into the SQWL trapping into the QWR region by overcoming the necking barrier before recombination in the SQWL. These results show that the QWR has strong lateral confinement from the necking quantum well after treatment by ion implantation.

3.3. Magneto-resistance of QWRs

In order to investigate the 1D electronic behavior in the QWRs and confirm further the improvement of the carrier accumulation in QWRs, we measured the magneto-resistance in two sets of configurations. First, the sample was rotated around the axis which lied in the substrate plane but was perpendicular to the wire orientation. The magneto-resistance for different tilted

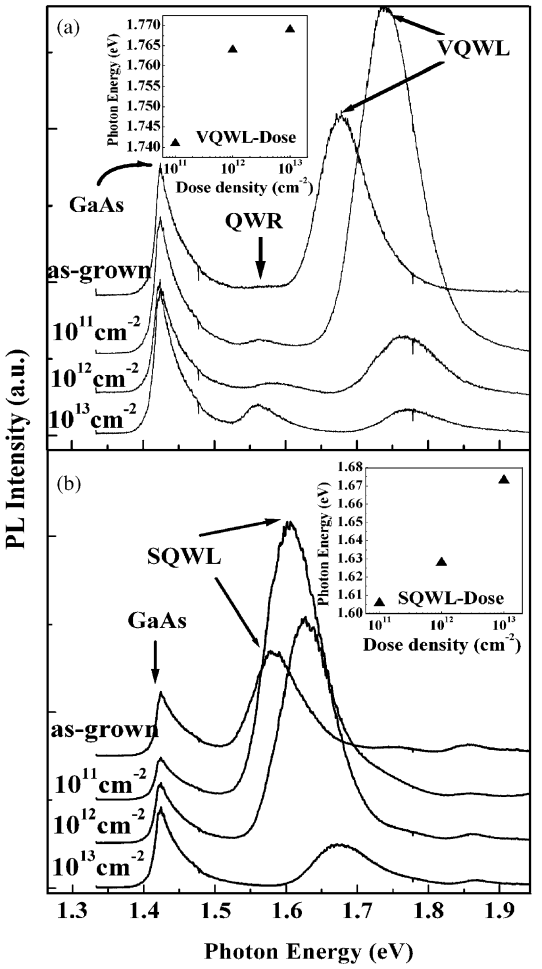

Fig. 3. (a) PL spectra for the QWR region, the inset is the ion implantation dose dependence of the peak energy of VQWL signal; (b) PL spectra for the SQWL region, the inset shows the ion implantation dose dependence of the peak energy of SQWL signal.

angles is plotted in Fig. 5(a). Second, we measured the magneto-resistance with the sample tilting around the axis along the wire direction. The results were displayed in Fig. 5(b). The measurement of configurations for both cases are also illustrated in the insets of the figures. The magneto-resistance in both cases shows no oscillation, different from the results obtained by Maciel et al. [10] and Tsukernik et al. [11]. Since the magneto-oscillation may correspond to the oscillatory screening effect of a dense 2D electron gas,

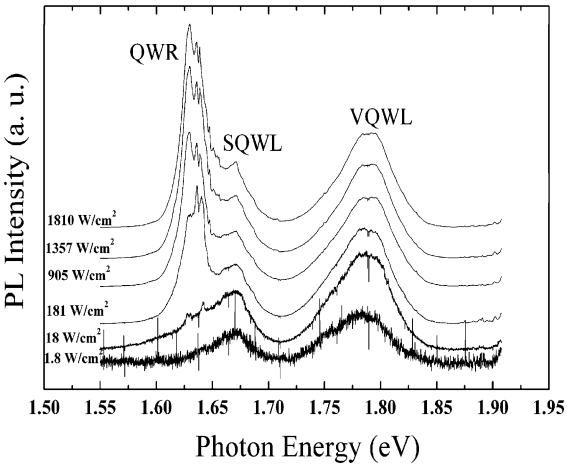

Fig. 4. Excitation power density dependence of the PL spectra at 4 K for the QWR sample with the ion implantation dose density of 10^{13} cm^{-2}, and the excitation wavelength was 633 nm.

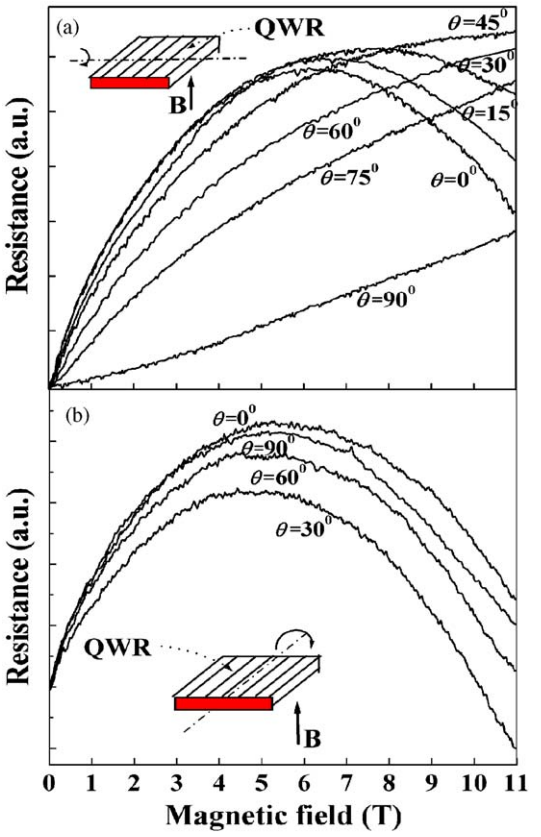

Fig. 5. Magnetic field dependence of the resistance of the QWR sample with the ion implantation dose density of 10^{13} cm^{-2}. The magnetic field configuration is for the sample shown as in the inset.

this implies that the electron accumulation and mobility in the SQWLs and VQWLs of our samples is less. In Fig. 5(a), the magnetic field dependence of sample resistance shows a maximum at $B \approx 5\,\mathrm{T}$ when the tilted angle of the wire orientation relative to the magnetic field is small ($<45^\circ$). The magnetic field corresponding to the maximum shifts to the higher magnetic field, i.e. $B \approx 5/\cos(\theta)\,\mathrm{T}$ while increasing the tilted angle. At 90°, the magnetic field dependence of the resistance curve becomes nearly linear in the range of 0–11 T. For the measurement configuration illustrated in Fig. 5(b), the sample resistance reaches a maximum at about 5 T. In this case, the QWR are always perpendicular to the magnetic field, whereas the angle between the SQWLs, VQWLs and the magnetic field changes, while rotating the sample. The resistance maximum hardly shifts, i.e. the tendency of the magnetoresistance for different tilted angles remains similar to the curve with 0° tilted angle as shown in Fig. 5(b). This phenomenon strongly suggests that the contribution from the electrons in VQWLs and SQWLs to the conductivity of the sample is small and the transport behavior mainly results from the electrons in QWRs.

4. Conclusions

In conclusion, the ion implantation followed by a RTA was introduced to improve the electron confinement in GaAs V-grooved QWRS. Spatially resolved PL results indicate that the ion-implantation-induced quantum well intermixing raises significantly the electron sub-band energies of the SQWL and VQWL. Processes of real space carrier transfer from the SQWL region into the QWR region showed the blocking effect of the necking quantum well region. Furthermore, a more efficient accumulation of electrons in QWRs is achieved. Our magneto-transport measurements on the ion-implanted QWR samples also suggest the quasi-1D motion of electrons in the structure.

Acknowledgments

This work is financially supported by the National Natural Science Foundation of China (no. 10374018, no. 10321003 and no. 90401015), the Scientific Committee of Shanghai (no. 03DJ14001), and the Special Funds for Major Basis State Research Project of China (Grant no. 2004CB619004).

References

[1] S.C. Shen, Spectroscopy and Optical Properties of Semiconductors, second ed., Science Publication, Beijing, 2002, p. 695.
[2] G. Biasil, E. Kapon, Y. Ducommun, A. Gustafsson, Phys. Rev. B 57 (1998) R9416.
[3] D.Y. Oberli, M.-A. Dupertuis, F. Reinhardt, E. Kapon, Phys. Rev. B 59 (1999) 2910.
[4] L. Sirigu, D.Y. Oberli, L. Degiorgi, A. Rudra, E. Kapon, Phys. Rev. B 61 (2000) R10575.
[5] D. Kaufman, Y. Berk, B. Dwir, A. Rudra, A. Palevski, E. Kapon, Phys. Rev. B 59 (1999) R10433.
[6] R. Bhat, E. Kapon, D.M. Hwang, M.A. Koza, C.P. Yun, J. Cryst. Growth 93 (1989) 850.
[7] X.L. Wang, M. Ogura, H. Matsuhata, Appl. Phys. Lett. 67 (1995) 804.
[8] Z.F. Li, The spectra studies of semiconductor functional materials, National Laboratory for Infrared Physics, Shanghai Institute of Technical Physics, Chinese Academy of Sciences, 2001, p. 45.
[9] E. Kapon, D.W. Hwang, R. Bhat, Phys. Rev. Lett. 63 (1989) 430.
[10] A.C. Maciel, J. Kim, J.F. Ryan, Solid-state Electron 42 (1998) 1245.
[11] A. Tsukernik, A. Palevski, V.J. Goldman, S. Luryi, E. Kapon, A. Rudra, Phys. Rev. B 63 (2001) 153315.